Original

Soto-Alvaredo, J.; Dutschke, F.; Bettmer, J.; Montes-Bayon, M.; Proefrock, D.; Prange, A.:

Initial results on the coupling of sedimentation field-flow fractionation (SdFFF) to inductively coupled plasma-tandem mass spectrometry (ICP-MS/MS) for the detection and characterization of TiO2 nanoparticles

In: Journal of Analytical Atomic Spectrometry (2016) Royal Society of Chemistry

DOI: 10.1039/C6JA00079G

JAAS

TECHNICAL NOTE

View Article Online
View Journal | View Issue

Cite this: *J. Anal. At. Spectrom.*, 2016, **31**, 1549

Initial results on the coupling of sedimentation field-flow fractionation (SdFFF) to inductively coupled plasma-tandem mass spectrometry (ICP-MS/MS) for the detection and characterization of TiO_2 nanoparticles†

Juan Soto-Alvaredo,‡[ab] Florian Dutschke,‡[b] Jörg Bettmer,*[a] María Montes-Bayón,[a] Daniel Pröfrock*[b] and Andreas Prange[b]

Received 3rd March 2016
Accepted 25th April 2016

DOI: 10.1039/c6ja00079g

www.rsc.org/jaas

Manufactured TiO_2 nanoparticles (TiO_2 NPs) are nowadays widely present in products accessible to the mass market like paints, cosmetics or sunscreens. Despite the great increase in the use of these nanoparticles, until now their potential effects on the environment and biological systems have not been sufficiently studied. Reliable analytical methods are therefore required for better characterization of these emerging materials. We suggest the hyphenation of inductively coupled plasma-mass spectrometry (ICP-MS) with a separation technique like sedimentation field-flow fractionation (SdFFF) to obtain information related to the size and state of agglomeration of the investigated nanoparticles. In this work, initial experiments related to the on-line coupling of SdFFF to inductively coupled plasma-tandem mass spectrometry (ICP-MS/MS) have been conducted allowing the detection and separation of TiO_2 NPs. The application of the ICP-MS/MS technology using a NH_3 mass shift mode allowed the removal of the different molecular and isobaric interferences that complicate the reliable detection and quantification of Ti. Under optimised conditions, the achievable instrumental detection limits in matrix solutions were below 10 ng L^{-1} of Ti. The separation parameters of the SdFFF system were optimized using two commercially available model TiO_2 NPs (nominal sizes: 21 and 50 nm). These materials were characterised concerning hydrodynamic diameters and the state of aggregation also using a multiangle light scattering (MALS) analysis detector. A transmission electron microscopy (TEM) technique was also applied to confirm the sizes and the shapes of the TiO_2 NPs as well as the presence of aggregates. To demonstrate the applicability of the combination of SdFFF and ICP-MS/MS for the detection of TiO_2 NPs at trace levels as well as to gain information about their hydrodynamic diameter and agglomeration state, the optimized method has been applied to the analysis of real water samples from a local lake in Germany.

Introduction

Nanotechnology has greatly developed during the last decade, being nowadays more than a promising technological revolution in our society. In particular, manufactured TiO_2 NPs are one of the most produced and applied nanomaterials for industrial applications. Some experts estimate the annual European TiO_2 NP production and usage to be 10 000 t or even higher.[1] TiO_2 NPs are indeed nowadays widely present in products accessible to the mass market like paints, food additives or personal care products like toothpaste or sunscreen,[2] and it is also widely used *e.g.* in water purification systems. Between 70 and 80% of the whole production of nano-sized TiO_2 is applied to the manufacturing of cosmetics; TiO_2 is the only inorganic UV filter permitted in sunscreens with a maximum allowable product concentration of up to 25% (w/w).[3] TiO_2 is also used as an abrasive and antibacterial agent[4] and therefore present in toothpastes and many other pharmaceutical products. Consequently, unknown quantities of TiO_2 NPs enter the environment, primarily through industrial and sewage wastewater discharges.[5,6]

However, this technological progress might also be associated with certain risks. The small size of engineered

[a]*Department of Physical and Analytical Chemistry, University of Oviedo, C/Julian Clavería 8, 33006, Oviedo, Spain. E-mail: bettmerjorg@uniovi.es*

[b]*Department of Marine Bioanalytical Chemistry, Helmholtz-Zentrum Geesthacht, Zentrum für Material- und Küstenforschung, Max Planck Str. 1, 21502 Geesthacht, Germany. E-mail: daniel.proefrock@hzg.de*

† Electronic supplementary information (ESI) available. See DOI: 10.1039/c6ja00079g

‡ These two authors contributed equally to the present work.

nanomaterials can increase adverse toxicological effects in living organisms, since nanoparticles are able to pass through the cellular membranes, and therefore, to enter eukaryotic cells. By using transmission electron microscopy (TEM), the uptake of TiO_2 NPs has been observed and evaluated in many different cellular cultures like HT29 (human enterocytes), Caco-2 (epithelial human cells) or RajiB cells (hematopoietic human cells) among many others.[7,8] Furthermore, there are several *in vitro* studies regarding the toxicity of TiO_2 NPs in human cells, reporting that they can potentially produce oxidative stress, inflammatory responses, apoptosis,[9] DNA damage,[10] or genotoxicity[11] to cells and tissues.

All these facts increase concerns about the fate and accumulation of these particles, their degradation, potential toxicity and potential risks to the environment, biological systems and finally the human health. The possible impact on aquatic species and the marine food chain, particularly algae and zooplankton, and their effects on the aquatic environment still have not been studied sufficiently.[12] Hence, due to the potentially diverse toxicological effects of TiO_2 NPs on ecological systems, analytical methods are urgently required to provide reliable information about the concentration, composition, size distribution, state of aggregation and agglomeration and presence of the corresponding metal ions detached from the particles.

Among the available analytical techniques, inductively coupled plasma-mass spectrometry (ICP-MS) offers quantitative element determination with high selectivity, high sensitivity and low detection limits that would enable the detection of TiO_2 NPs at trace concentration levels *via* their Ti content.[13] However, important challenges affect the detection of Ti by ICP-MS in environmental and biological samples, mainly due to the isobaric and polyatomic interferences affecting all Ti isotopes (see Table S1†).

This challenge was typically solved by using high-resolution inductively coupled plasma-sector field-mass spectrometry (ICP-SF-MS)[14,15] and applying a resolving power of $R > 3000$. However, the use of a higher mass resolution always involves a decrease in the sensitivity. Additionally, when working in medium resolution, the most abundant isotope of Ti, ^{48}Ti, cannot be completely separated from the isobaric interference of ^{48}Ca. Nevertheless, by working at medium resolution the detection of Ti can be achieved without interferences using its isotopes ^{47}Ti and ^{49}Ti with detection limits around 0.05 μg L^{-1}.[15]

In 2014, Balcaen *et al.* proposed a new approach for the elimination of interferences of Ti based on the use of inductively coupled plasma-tandem mass spectrometry (ICP-MS/MS).[16] The selective combination of Ti with O_2 or NH_3/He as reaction gases inside the reaction cell forms product ions that allow the measurement of Ti in a shifted mass range, preventing the interferences due to their lack of reactivity with the selected reaction gases. This approach permits the detection of Ti in environmental and biological matrices while eliminating all typical matrix derived interferences, which results in improved detection limits below 0.02 μg L^{-1}.

Besides a sensitive and selective technique to detect Ti, a separation method to determine the TiO_2 NP particle size distribution is of high relevance. In this regard, field-flow fractionation is a family of separation techniques suitable for the separation of natural colloids, micro-size particles and NPs in solution.[17] Asymmetrical flow field-flow fractionation (AF4) has been applied for the separation of TiO_2 NPs present in cosmetics, food or sunscreens.[18–20] However, some drawbacks such as the membrane–particle interaction and the particle size-dependence recoveries make the straightforward application of AF4 for the separation of TiO_2 NPs difficult.[21]

Sedimentation field-flow fractionation (SdFFF) has been also applied to the separation and analysis of colloids[17,22,23] and it has been demonstrated to be a feasible technique to provide information about size distribution profiles of metal oxide nanoparticles like SiO_2[24] or TiO_2 NPs.[25–28]

In this work, initial studies on the online coupling of SdFFF with ICP-MS/MS will be conducted for the first time for the separation and detection of TiO_2 NPs. Following optimization of the ICP-MS/MS parameters for an efficient removal of isobaric and polyatomic interferences (see Table S1†), the coupling to SdFFF will be tested using Ag and TiO_2 NPs. In the case of TiO_2 NPs, the optimized method will provide preliminary information on the particle size distribution and agglomeration degree verified by transmission electron microscopy (TEM). Finally, the developed methodology will be applied to the analysis of TiO_2 NPs in lake water samples.

Materials and methods

Chemicals

ICP-Standards (Ti, Ag, Ca, Rh, and In, each 1.000 g L^{-1}) were purchased from Th. Geyer GmbH & Co. KG (Renningen, Germany). Polystyrene (PS) latex beads having nominal diameters of 125, 200, 300, and 600 nm were purchased from PostNova (Landsberg am Lech, Germany) and used for the MALS detector calibration. NanoXact Silver with diameter sizes of 30 nm, 60 nm and 100 nm (Ag-NPs) stabilized with citrate was purchased from Nanocomposix (Prague, Czech Republic) and was used for the optimization of the SdFFF system.

Sodium dodecyl sulfate (SDS) (Sigma Aldrich, St. Louis, USA) 0.1% (w/v), and 0.5% (v/v) Fl-70 (Thermo Fisher Scientific Inc., Waltham, USA) were used as carrier solution additives for the SdFFF system. All solutions were freshly prepared using MilliQ water (Millipore, Billerica, USA). HNO_3 was obtained from Merck (suprapur, Darmstadt, Germany). All solutions were filtered (0.2 μm pore size) before their utilization.

For the development of the SdFFF method for TiO_2 NPs, titanium dioxide (TiO_2) of 21 nm from Sigma Aldrich Germany (Degussa Aeroxide® P25 produced by Evonik Industry, Essen, Germany), TiO_2 of 50 nm from US Nano (US Research Nanomaterials, Houston, USA) and another 21 nm material (NIST SRM 1898) were used. A NASS4 seawater reference material (NRC, Otawa, Canada) was used in this work to simulate a seawater matrix.

Instrumentation

For the SdFFF, a centrifugal field-flow-fractionation system (CF2000 PostNova, Landsberg am Lech, Germany) with

a channel dimension of 576 mm length, 20 mm width and 250 μm height as well as a channel radius of 10.015 cm was used. For the on-line size and Ti determination, a MALS detector was coupled on line to the SdFFF system followed by an ICP-MS/MS Agilent 8800 (Agilent, Santa Clara, USA) equipped with a PFA 100 (for total Ti determinations) or PFA ST nebulizer as well as a Peltier-cooled Scott-type spray chamber. The ICP-MS/MS system comprises two quadrupoles and an octopole between them working as a collision/reaction cell. For these studies, O_2 and NH_3/He were tested separately as cell gases with respect to their reaction and product ion formation with different Ti isotopes.

A transmission electron microscope (TEM) JEM2000ExII (Jeol Ltd, Tokyo, Japan) operating at 180 kV has been used in this work to validate the size distribution profile obtained after the SdFFF separation and to provide additional information about the shape of the particles.

Sample preparation for TEM analysis

For the TEM experiments, a solution of tetrahydrofuran (THF) containing 5 mg mL^{-1} of each of the two samples of TiO_2 NPs was prepared and a few drops were put onto carbon coated copper grids. The grids were dried overnight inside a clean bench (Class 100) and stored isolated and preserved from light, until their examination by TEM microscopy.

Determination of Ti by ICP MS/MS

A methodology for the interference-free detection of Ti at trace levels using an ICP-MS/MS system (ICP-QQQ, Agilent 8800) was developed based on the work published by Balcaen *et al.*[16] In this work, NH_3/He was used as reaction gas. After selecting the masses of different Ti isotopes in the first quadrupole, the chosen reaction gas combines selectively with Ti (and not with its interfering ions) inside the reaction cell producing the product ions. They were selected in the second quadrupole as target masses. Detailed information can be found in the ESI.† The optimized parameters for Ti detection with the ICP-MS/MS system as well as the selected mass shifts are summarized in Table 1.

Separation of titanium dioxide nanoparticles (TiO_2) with SdFFF

In order to optimize the initial instrumental settings for the separation methodology for TiO_2 NPs, three silver nanoparticle (AgNP) standards with 30, 60 and 100 nm diameter sizes, respectively, were used as model nanoparticles with negligible agglomeration behaviour and a narrow size distribution of the particle nominal size.

For further optimization of this method, two different commercially available TiO_2 NP materials with nominal particle diameters of 21 and 50 nm were used. The suspensions of the particles were prepared in 0.05% (v/v) Fl-70 and were homogenised in an ultrasonic bath. The different instrumental parameters of the SdFFF system, like initial applied field strength, field programming or the equilibration time, were optimized using these materials. The optimized parameters for the SdFFF separations are shown in Table 1.

Table 1 Applied instrumental conditions for ICP-MS/MS and SdFFF instruments

ICP-MS/MS instrumental conditions	
Reaction gas	NH_3/He
Scan type	MS/MS
RF power	1550 W
Carrier gas flow rate	1.07 L min^{-1}
Reaction gas flow rate	2 mL min^{-1}
Q1 bias	−1 V
Octopole bias	−5 V
Energy discrimination	−8 V
Q2 bias	−13 V
Q2 axis offset	−0.01V
Q1 masses (u)	46, 47, 48, 49, 50
Q2 masses: (mass shifts from each Ti isotope)	+15, +32, +49, +66, +84, +102
Wait time offset	2 ms
SdFFF instrumental conditions	
Channel flow rate	0.5 mL min^{-1}
Equilibration time	10 min
Initial applied field	1000 rpm
Power field programming	$t_1 = 8$ min (focus time at the initial field), and $t_a = -64$ (field decay parameter)
Final field	50 rpm

The absolute recovery (rec_{SdFFF}) of the samples was calculated using the channel bypass method.[29] Again, three different eluents were evaluated in order to investigate their influence on the absolute recovery: water, 0.05% (v/v) Fl-70 and 0.05% (w/v) SDS.

Then, to determine quantitative recovery, the centrifuge speed was set to 0 rpm and the recovery rate was calculated from the comparison of the area with (A_{SdFFF}) and without (A_0) centrifugation speed (see eqn (1)).

$$rec_{SdFFF} = \frac{A_{SdFFF}}{A_0} \times 100\% \quad (1)$$

In any case, the recovery rates were determined with both, MALS and ICP-MS/MS detection.

Results and discussion

Separation method for TiO_2 nanoparticles

At a certain concentration, TiO_2 NPs are usually present as agglomerates instead of single particles in water samples.[30] This fact does not permit us to obtain a narrow peak for the separation of these particles using the SdFFF. Therefore, in order to optimize the system, three different silver nanoparticles (AgNPs) with 30, 60, and 100 nm diameter sizes were used for the evaluation of the instrumental parameters for the separation with SdFFF as well as standards for the size calibration of this separation technique.

The flow rate was set to 0.5 mL min^{-1}, as this is the optimal flow rate of the nebulizer used for the coupling with the ICP-MS/MS system (PFA ST nebulizer). Changes in the relaxation time as well as in the focus time from 5 to 10 min did not show any impact on the separation. Five different initial field strengths were tested corresponding to a centrifugation setting of 1000, 2000, 3000, 4000 and 4900 rpm. This parameter did not show any influence on the resolution of Ag NPs. In order to minimize the total analysis time, 1000 rpm was used for the following experiments. Further operating conditions can be found in Table 1.

These experimental conditions were used for the analysis of two TiO_2 NPs with nominal diameters of 21 and 50 nm, respectively. Due to the mentioned trend of TiO_2 NPs to form aggregates and agglomerates in water solution that resulted in their sedimentation on the bottom of the vials, it was difficult to get reliable concentrations and repeatable results during the analysis. Therefore, the influence of the composition of the solubilization solution as well as the carrier chosen for the SdFFF technique was evaluated. For this purpose, two different surfactants (SDS and Fl-70) were chosen as additives in the sample solution in order to improve the stability of the suspension over time. The presence of Fl-70 provided best results and after its addition, the NPs remained suspended over the time of the experiment; so subsequent experiments were thereby carried out using this stabilizing agent at a concentration of 0.05% (v/v).

The presence of surfactants as carrier additives could compromise the sensitivity of the detection systems for the NPs. Therefore, the SdFFF was coupled to MALS and ICP-MS/MS in order to address the effect of the different carrier solutions on the separation/detection of 50 nm TiO_2 NPs. Fig. 1 reveals that the presence of SDS results in fractograms with much lower intensity and lower signal-to-noise ratio in both detectors. FI-70 had no influence on the detected signal by MALS but a significant decrease (~30%) in the signal detected by the ICP-MS/MS. Pure water as a carrier, though, showed an improvement in both the stability of the signal and the sensitivity (see Fig. 1), and better recoveries (see Table 2) in comparison to Fl-70 and SDS. This finding suggested that even when the presence of surfactants improves the stability of the suspended NPs, its detrimental effect on the nebulization or transport efficiency of Ti does not recommend its use in the carrier solution in ICP-MS/MS detection. Therefore, further experiments were carried out using FL-70 only for stabilization of the samples, while for all separations MilliQ water has been used as carrier solution.

Fig. 2 shows the size distribution of the two TiO_2 NPs obtained by the mathematical conversion of time (Fig. 2A) into size (Fig. 2B) with the SdFFF theory (see ESI†). These results confirmed that the particles with a nominal size of 21 and 50 nm, respectively, exhibit final sizes with a size distribution profile ranging from their nominal size to sizes around 300 and 400 nm, and a maximum of population at 150 and 250 nm, respectively. The images obtained by transmission electron microscopy (TEM, see Fig. 2A) also show this aggregation/agglomeration tendency. The histograms obtained from the TEM images ($n = 30$) showed a mean size of the particles laying

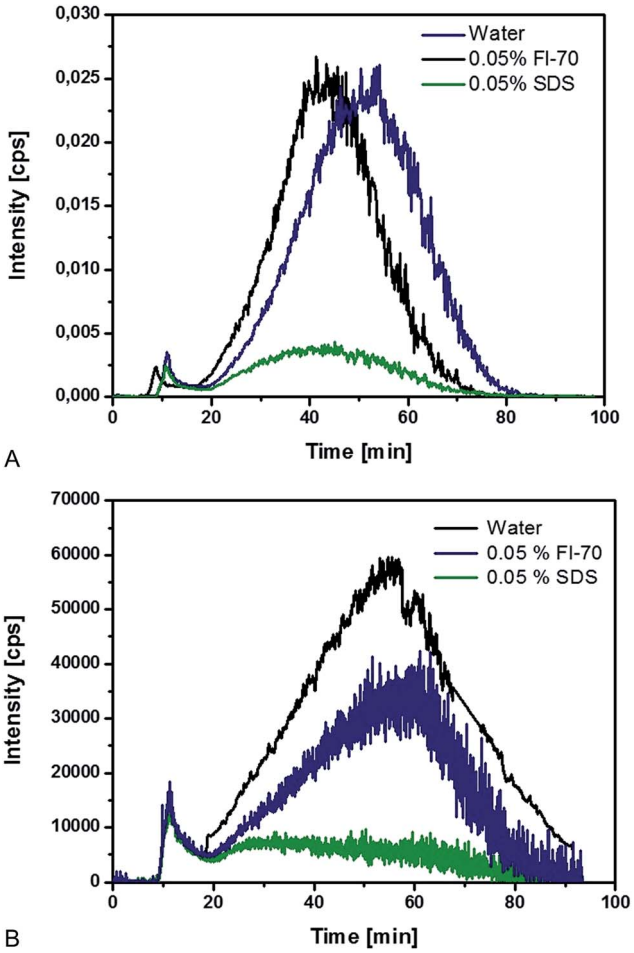

Fig. 1 Influence of different eluents in the SdFFF separation on the fractograms of 21 nm TiO_2 NPs detected (A) by MALS and (B) by ICP-MS/MS (*m/z* in Q1: 48, *m/z* in Q2: 150) detection.

Table 2 Absolute recovery calculated by the channel bypass method

Initial field strength		Recovery @ 1000 rpm (%)	Recovery @ 2500 rpm (%)
ICP-MS/MS detection	Milli Q	88.3	83.0
	Fl-70	50.1	53.3
	SDS	15.5	14.1
MALS detection	Milli Q	75.4	68.9
	Fl-70	40.8	48.5
	SDS	8.4	13.6

around 250 nm for the 21 nm TiO_2, and 150 nm for the 50 nm TiO_2 (see Fig. S2 and S3 in ESI†) confirming the size distribution results obtained by the SdFFF–MALS analysis.

The repeatability of the signals obtained by ICP-MS/MS detection was tested for the injection of 20 μg L^{-1} of 21 nm TiO_2 (NIST SRM 1898) NPs giving a standard deviation of 3.5% for the peak area ($n = 5$). Calibration using the same material showed good linearity ($R^2 = 0.992$) with a sensitivity of 2.93×10^6 L cps mg^{-1}. The calculated detection limit was 6.8 μg L^{-1} (3s-criterion). Therefore, a pre-concentration step might be advisable when analysing environmental samples with this system and

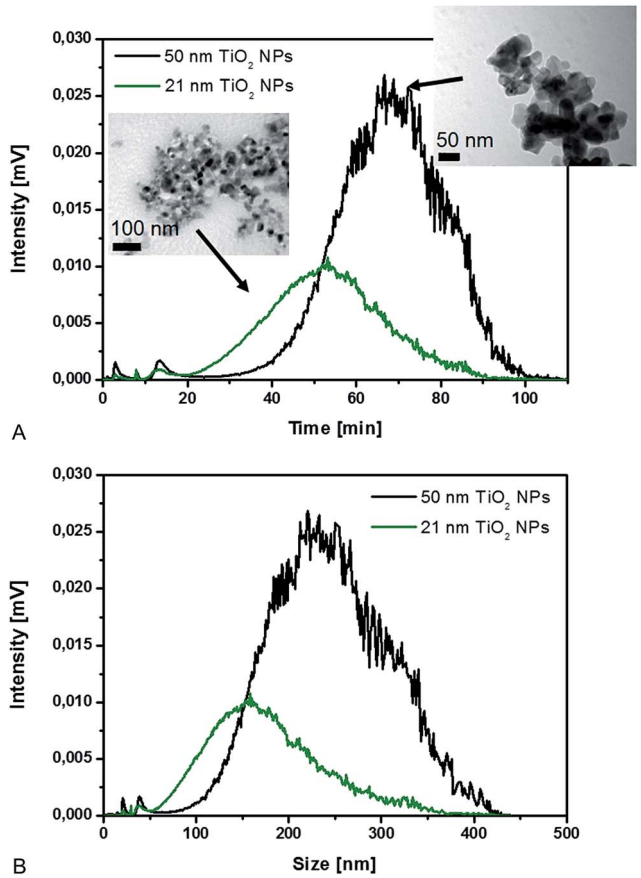

Fig. 2 Conversion (by means of the FFF theory) of retention times (A) into the size distribution profile (B) after the analysis of the investigated TiO_2 NPs by SdFFF coupled to MALS detection (insets: TEM images of the investigated TiO_2 NPs).

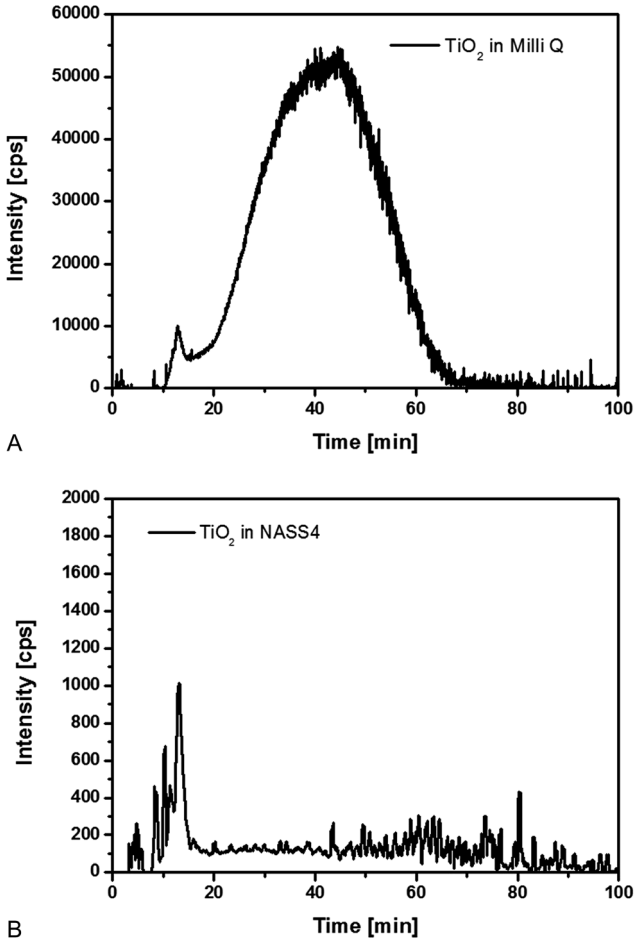

Fig. 3 Analysis of TiO_2 NP spiked samples of (A) MilliQ, and (B) NASS4 seawater reference material by SdFFF-ICP-MS/MS (*m/z* in Q1: 48, *m/z* in Q2: 150).

under the here given working conditions in order to improve the particle detection.

Application of the method to spiked and unspiked water samples

The developed methodology was tested for its application to the characterization of TiO_2 NPs in seawater samples. With this aim, two water samples: MilliQ and NASS4 (Fig. 3A and B, respectively) were injected into the system after spiking them with 21 nm TiO_2 NPs for a final concentration of 4 mg L^{-1}. By comparing the fractograms shown in Fig. 3, it is possible to address the matrix influence. Only unspecific signals for Ti were observed in the case of the seawater sample while the NPs can be detected in MilliQ water. This finding is in accordance with French *et al.*[31] who reported a strong influence of the ionic strength on the aggregation of TiO_2 NPs. The authors report that an ionic strength of only 0.009 mol L^{-1} already produced large aggregates of TiO_2 NPs in the 1 to 10 μm size range that sediment over time. Seawater with an ionic strength of approximately 0.7 mol L^{-1} would have presumably much stronger aggregation behaviour leading to the fast sedimentation of the particles.

In river or lake waters, the expected ionic strengths, however, range from 0.001 to 0.005 mol L^{-1}, so that a lower aggregation effect could be expected. Consequently, a representative sample was taken from the lake "Hohendeicher See" in the north of Germany, which is a highly frequented recreational area near Hamburg, to demonstrate the applicability of the methodology.

Therefore, 500 mL of the lake water sample (without spiking any TiO_2 NPs) were acidified with 3 mL sub-boiled HNO_3 65% for preservation. One aliquot was directly injected into the SdFFF system without any other treatment than sonication (10 min). A second sample was pre-concentrated by centrifugation at 10 000 rpm during 2 h. Fig. 4 represents the resulting fractograms of the two differently treated samples, already converted into the size distribution. In both cases, it was possible to detect Ti NPs with a broad size distribution of the detected particles which was equivalent (in the range of ~75–400 nm). In addition, it is possible to observe that the pre-concentrated sample shows higher intensity than the one without any pre-concentration. However, this study cannot clarify the origin of the observed TiO_2 NPs. Either the use of TiO_2-containing sunscreens or lake sediments containing TiO_2 suspended by human activity can cause the high abundance of

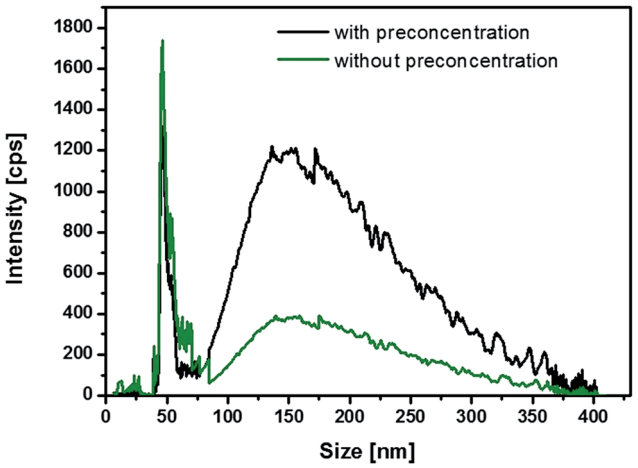

Fig. 4 TiO_2 NP detection and characterization by SdFFF-ICPMS/MS (m/z in Q1: 48, m/z in Q2: 150) in a real lake water sample taken from the Hohendeicher Lake (Hamburg, Germany).

TiO_2 in the samples. In any case, the developed methodology showed potential for the analysis of Ti NPs in environmental samples and should be further explored for future applications in environmental analysis.

Conclusions

In this work, we suggest the application of coupling SdFFF with ICP-MS/MS for the analysis of TiO_2 NPs. Experimental parameters for the SdFFF were optimized on the use of different Ag and TiO_2 NPs. Most decisive factors for a successful analysis of TiO_2 NPs were the composition of the carrier solution and the sample composition itself. Milli Q water gave best results in terms of detection sensitivity as a carrier, whereas FL-70 was chosen for the stabilisation of the particle suspensions. Initial experiments on the analysis of different water samples (Milli Q water, seawater, and a sample from a lake) showed a strong influence of the ionic strength on the analysis of TiO_2 NPs. Seawater containing high salt concentrations resulted in a pronounced aggregation/agglomeration with subsequent sedimentation as already reported in the literature.[31] However, the analysis of lake water with relatively low ionic strength resulted in the detection of TiO_2 NPs in the size range between ~75 and 400 nm.

This preliminary study demonstrated that the coupling of SdFFF to ICP-MS/MS might be a prospective tool for the analysis of TiO_2 NPs in environmental samples and probably also for other NP materials based on metal oxides.

Acknowledgements

J. Soto-Alvaredo acknowledges the fellowship from the Helmholtz-Zentrum, Geesthacht, and J. Bettmer gratefully acknowledges the financial support from the Spanish MICINN (Spanish ministry for science and innovation, Grant Number CTQ2011-23038) and from the FICYT (Grant number: FC-15-GRUPIN14-010).

References

1 F. Piccinno, F. Gottschalk, S. Seeger and B. Nowack, *J. Nanopart. Res.*, 2012, **14**, 1–11.
2 A. Weir, P. Westerhoff, L. Fabricius, K. Hristovski and N. von Goetz, *Environ. Sci. Technol.*, 2012, **46**, 2242–2250.
3 A. Salvador and A. Chisvert, *Anal. Chim. Acta*, 2005, **537**, 1–14.
4 J. W. Liou and H. H. Chang, *Arch. Immunol. Ther. Exp.*, 2012, **60**, 267–275.
5 European Commission DG ENV, *News Alert Issue 278*, 2012, p. 2012.
6 R. J. Miller, S. Bennett, A. a. Keller, S. Pease and H. S. Lenihan, *PLoS One*, 2012, **7**, 1–7.
7 E. Brun, F. Barreau, G. Veronesi, B. Fayard, S. Sorieul, C. Chanéac, C. Carapito, T. Rabilloud, A. Mabondzo, N. Herlin-Boime and M. Carrière, *Part. Fibre Toxicol.*, 2014, **11**, 1–16.
8 J. Soto-Alvaredo, E. Blanco, J. Bettmer, D. Hevia, R. M. Sainz, C. López Cháves, C. Sánchez, J. Llopis, A. Sanz-Medel and M. Montes-Bayón, *Metallomics*, 2014, **6**, 1702–1708.
9 K. Becker, S. Schroecksnadel, S. Geisler, M. Carriere, J. M. Gostner, H. Schennach, N. Herlin and D. Fuchs, *Food Chem. Toxicol.*, 2014, **65**, 63–69.
10 K. T. Kitchin, R. Y. Prasad and K. Wallace, *Nanotoxicology*, 2011, **5**, 546–556.
11 J. Petković, B. Žegura and M. Filipič, *J. Phys.: Conf. Ser.*, 2011, **304**, 012037.
12 D. Minetto, G. Libralato and A. Volpi Ghirardini, *Environ. Int.*, 2014, **66**, 18–27.
13 K. J. Orians, E. A. Boyle and K. W. Bruland, *Nature*, 1990, **348**, 322–325.
14 A. Sarmiento-González, J. M. Marchante-Gayón, J. M. Tejerina-Lobo, J. Paz-Jiménez and A. Sanz-Medel, *Anal. Bioanal. Chem.*, 2005, **382**, 1001–1009.
15 Y. Nuevo-Ordóñez, M. Montes-Bayón, E. Blanco-González, J. Paz-Aparicio, J. D. Raimundez, J. M. Tejerina, M. A. Peña and A. Sanz-Medel, *Anal. Bioanal. Chem.*, 2011, **401**, 2747–2754.
16 L. Balcaen, E. Bolea-Fernandez, M. Resano and F. Vanhaecke, *Anal. Chim. Acta*, 2014, **809**, 1–8.
17 J. C. Giddings, *Science*, 1993, **260**, 1456–1465.
18 V. Nischwitz and H. Goenaga-Infante, *J. Anal. At. Spectrom.*, 2012, **27**, 1084–1092.
19 I. López-Heras, Y. Madrid and C. Cámara, *Talanta*, 2014, **124**, 71–78.
20 R. J. B. Peters, G. Van Bemmel, Z. Herrera-Rivera, J. P. F. G. Helsper, J. P. Hans, S. Weigel, P. Tromp, A. G. Oomen, A. Rietveld and H. Bouwmeester, *J. Agric. Food Chem.*, 2014, **62**, 6285–6293.
21 N. Bendixen, S. Losert, C. Adlhart, M. Lattuada and A. Ulrich, *J. Chromatogr. A*, 2014, **1334**, 92–100.
22 G. Karaiskakis, K. a. Graff, K. D. Caldwell and J. C. Giddings, *Int. J. Environ. Anal. Chem.*, 1982, **12**, 1–15.
23 J. J. Kirkland, W. W. Yau and F. C. Szoka, *Science*, 1982, **215**, 296–298.
24 C. Contado, L. Ravani and M. Passarella, *Anal. Chim. Acta*, 2013, **788**, 183–192.

25 P. J. P. Cardot, S. Rasouli and P. Blanchart, *J. Chromatogr. A*, 2001, **905**, 163–173.
26 A. Samontha, J. Shiowatana and A. Siripinyanond, *Anal. Bioanal. Chem.*, 2011, **399**, 973–978.
27 C. Contado and A. Pagnoni, *Anal. Methods*, 2010, **2**, 1112–1124.
28 C. Contado and A. Pagnoni, *Spectrosc. Eur.*, 2011, **23**, 6–12.
29 M. E. Schimpf, K. Caldwell and J. C. Giddings, *Wiley: Field-flow Fractionation Handbook*, John Wiley & Sons, New York, 2000.
30 J. J. Doyle, V. Palumbo, B. D. Huey and J. E. Ward, *Water, Air, Soil Pollut.*, 2014, **225**, 2106.
31 R. A. French, A. R. Jacobson, B. Kim, S. L. Isley, R. L. Penn and P. C. Baveye, *Environ. Sci. Technol.*, 2009, **43**, 1354–1359.